Table of Content

Figure S1

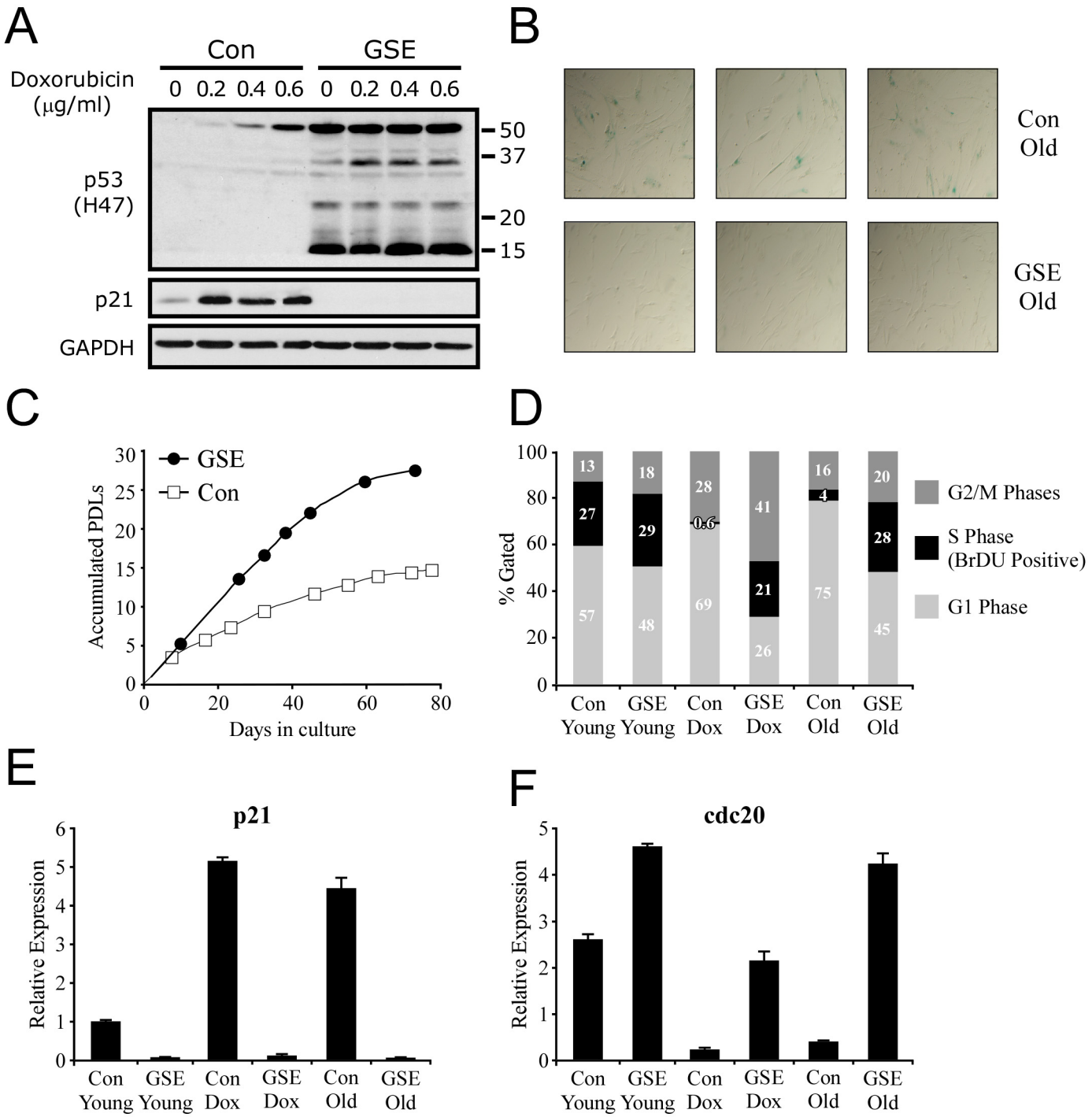
A
Con
GSE
Doxorubicin (μg/ml)
0 0.2 0.4 0.6 0 0.2 0.4 0.6
p53 (H47)
p21
GAPDH
50
37
20
15
B
Con Old
GSE Old
C
GSE
Con
Accumulated PDLs
Days in culture
D
% Gated
G2/M Phases
S Phase (BrDU Positive)
G1 Phase
Con Young
GSE Young
Con Dox
GSE Dox
Con Old
GSE Old
E
p21
Relative Expression
F
cdc20
Relative Expression

Figure S1. **Establishment of the WI-38 system.**
WI-38 primary human fibroblasts were infected with a retrovirus encoding for the p53-inactivating peptide, GSE56. These cells (GSE) and their active p53 counterparts (Con) were treated with the DNA damaging agent doxorubicin as well as grown until the onset of replicative senescence. A. Western blot depicting p53 and p21 following doxorubicin treatment. p53 was stabilized and activated its target gene p21 in the NEO cells upon treatment. In the GSE cells, p53 was stabilized in its inactive form already at basal levels by GSE56, a 15 kDa peptide detected by the H-47 anti-p53 polyclonal antibody. The p21 protein was not detectable in the GSE cells at basal levels, nor was it induced upon DNA damage, indicating of a complete inactivation of p53 transactivation activity. B and C. Introduction of the GSE56 peptide at passage 20 resulted in accelerated growth rate (C) and delay in replicative senescence, as indicated by the reduction of senescence-associated -galactosidase (SA- -Gal) staining (B). D. Cell cycle analysis demonstrates that both DNA damage and replicative senescence resulted in a sharp p53-dependent cell cycle arrest. E. QRT-PCR analyses of p21 mRNA levels demonstrated that p53 transactivation activity was significantly induced upon both DNA damage and replicative senescence, and was completely abolished by the introduction of GSE56. F. QRT-PCR analyses of cdc20, a p53-repressed gene that participates in cell-cycle progression. To conclude, we have generated an isogenic pair of primary human cell cultures that display p53-dependent cell cycle arrest, gene activation and repression, and senescence phenotypes upon application of p53-activating stress. Data are represented as mean ± SD.

Figure S2

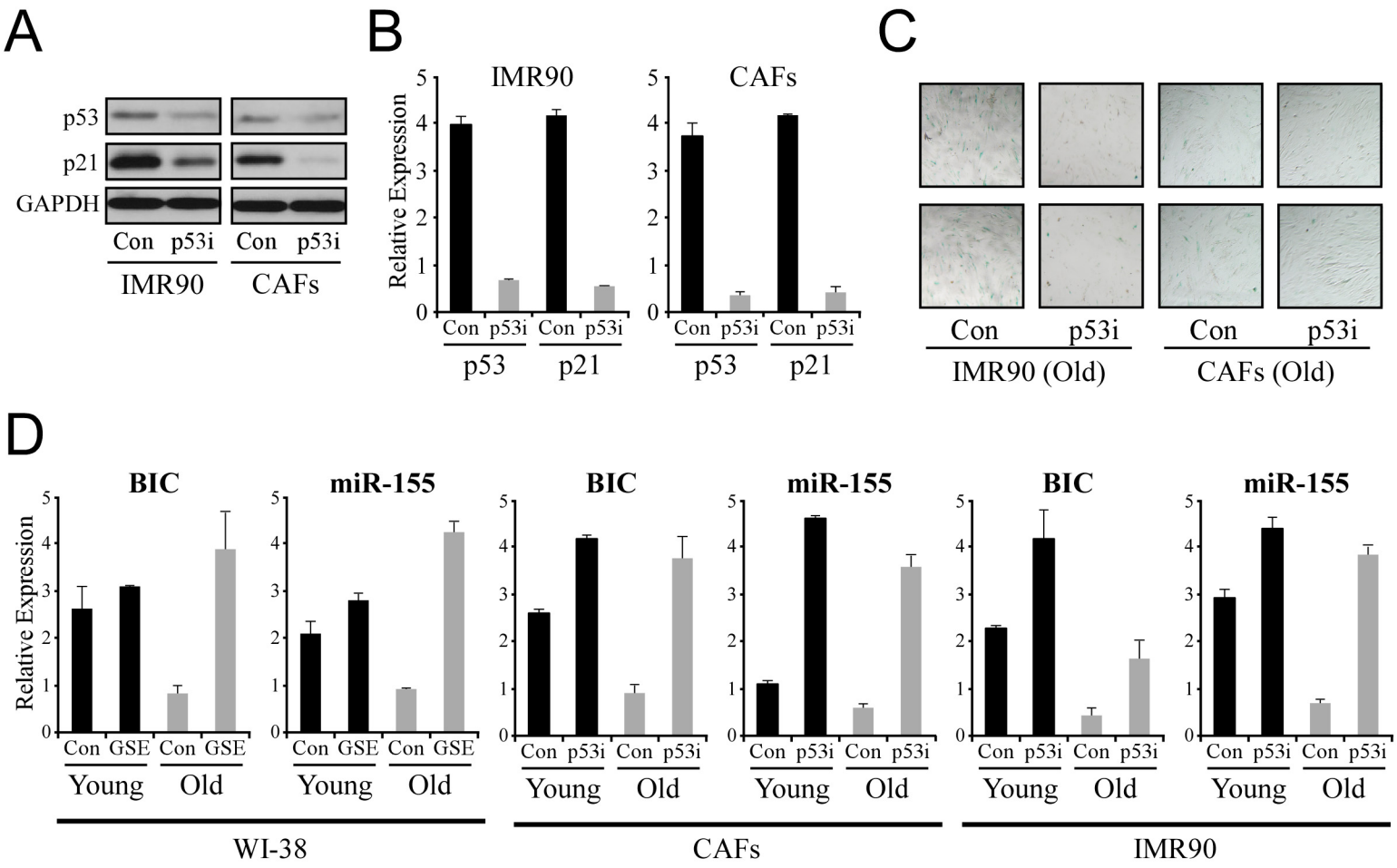

Figure S2. **Establishment of the IMR90 and CAFs systems.** Lung primary human fibroblasts IMR90 and prostate-cancer associated fibroblasts (CAFs) PFCA179 were infected with a retrovirus encoding for either a small hairpin RNA targeting p53 (p53i) or a control RNAi (Con), and grown until the onset of replicative senescence. A. A Western blot depicting p53 and p21 downregulation upon the stable expression of the p53 small hairpin RNA. B. QRT-PCR analyses of p53 and p21 mRNA levels. C. SA- -Gal staining for late passage IMR90 and CAFs. D. QRT-PCR analysis for the non-coding RNA BIC and its resident miRNA miR-155 in WI-38, CAFs and IMR90 cells. Samples were collected from early passage cultures (Young) and from late passage cultures (Old). Data are represented as mean ± SD.

Figure S3

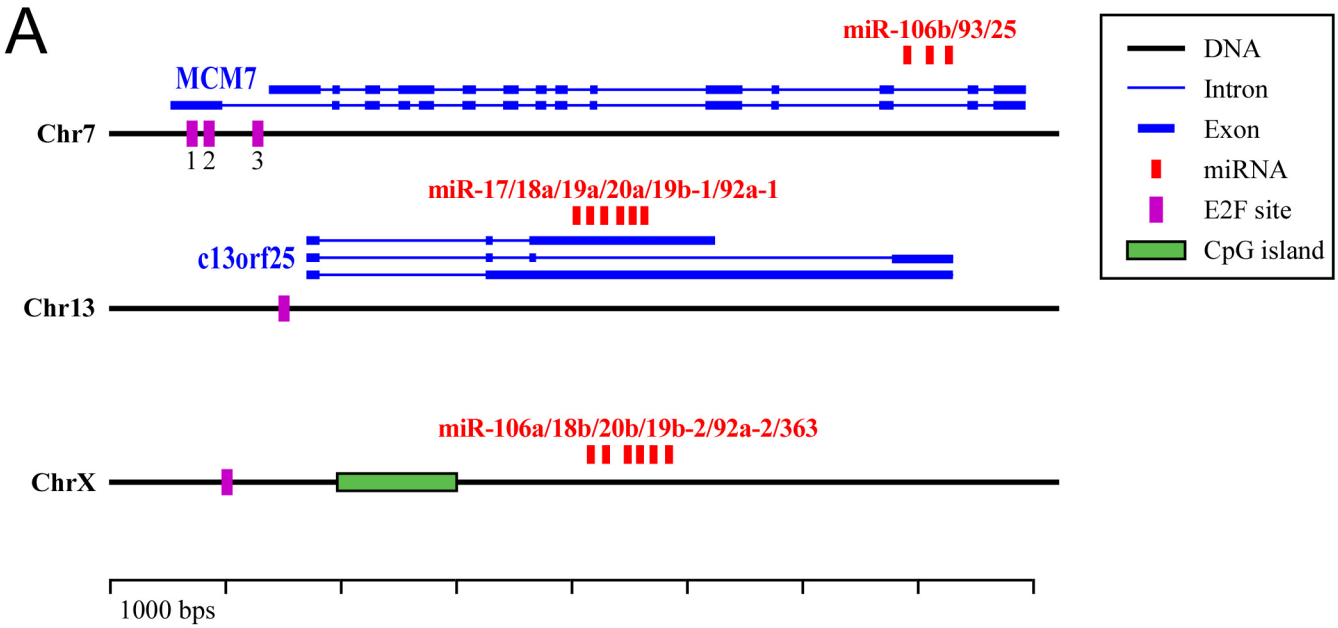
A
miR-106b/93/25
MCM7
Chr7
1 2 3
miR-17/18a/19a/20a/19b-1/92a-1
c13orf25
Chr13
miR-106a/18b/20b/19b-2/92a-2/363
ChrX
1000 bps
DNA
Intron
Exon
miRNA
E2F site
CpG island

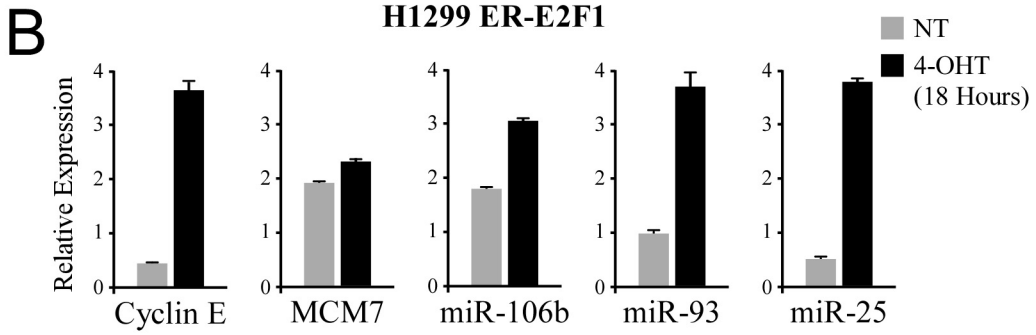
B
H1299 ER-E2F1
NT
4-OHT
(18 Hours)
Relative Expression
Cyclin E
MCM7
miR-106b
miR-93
miR-25

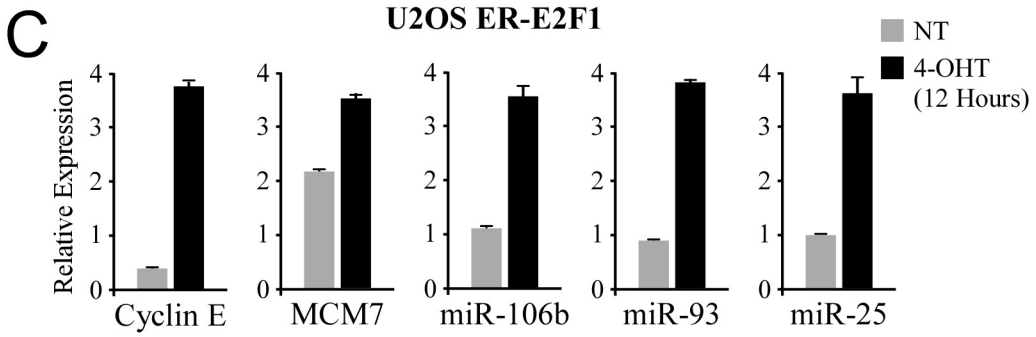
C
U2OS ER-E2F1
NT
4-OHT
(12 Hours)
Relative Expression
Cyclin E
MCM7
miR-106b
miR-93
miR-25

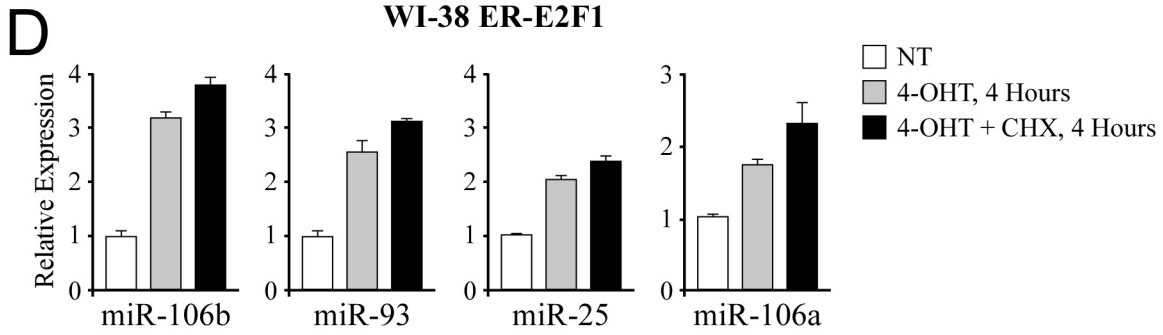
D
WI-38 ER-E2F1
NT
4-OHT, 4 Hours
4-OHT + CHX, 4 Hours
Relative Expression
miR-106b
miR-93
miR-25
miR-106a

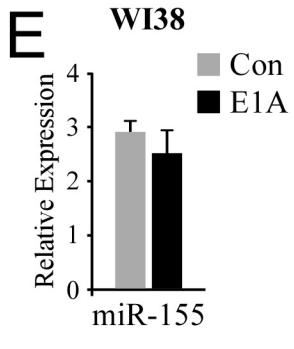
E
WI38
Con
E1A
Relative Expression
miR-155

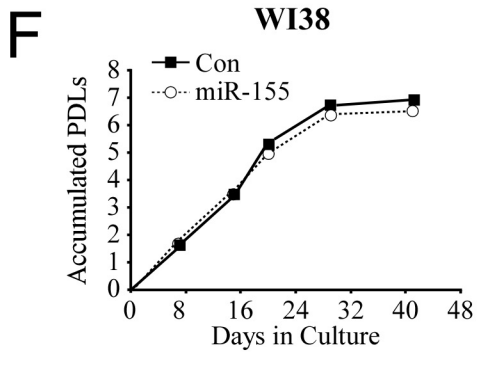
F
WI38
Con
miR-155
Accumulated PDLs
Days in Culture

Figure S3. The cell-cycle associated polycistronic miRNAs are directly induced by E2F.

A. Schematic representation of the genomic organization of the three paralogous polycistrons. Conserved E2F sites (according to the tfbsConsSites track from the UCSC database) are located upstream of each of the miRNA clusters. For the miR-106b-25 cluster, three E2F sites are found within 1kb upstream of MCM7 TSS. For miR-17-92 cluster, an E2F site is located 83 bps upstream of c13orf25 TSS. For miR-106a-92 cluster, which has no known host transcript, an E2F site is located upstream of a CpG island, indicative of a potential TSS in that region. ChIP analysis indicates binding of E2F1 to each of the E2F sites presented here (Fig. 4A). B and C. E2F induces the levels of miR-106b/93/25 polycistron. H1299 lung carcinoma cell line (A) and U2OS osteosarcoma cell line (B) were treated with 4-OHT for the indicated time periods. QRT-PCR analyses demonstrated upregulation of the known E2F1 target, Cyclin E; as well as of MCM7 and its resident miRNAs. D. ER-E2F1 expressing WI-38 cells were treated with 4-OHT (300nM) in combination with 80 g/ml of cycloheximide (CHX) for 4 hours. The levels of the polycistronic miRNAs were measured by QRT-PCR. Note that cycloheximide did not attenuate the induction of the miRs by 4-OHT, indicating that the transactivation of the miRs by E2F1 does not require the synthesis of a protein mediator. E. WI-38 cells were infected with the oncoprotein E1A or a control vector (Con) and QRT-PCR analysis was performed to measure the level of miR-155. F. Growth curves for control (empty vector) and miR-155 overexpressing cells. Both cell types displayed comparable growth rate and entered replicative senescence simultaneously. PDLs = Population Doublings. Data are represented as mean ± SD.

Figure S4

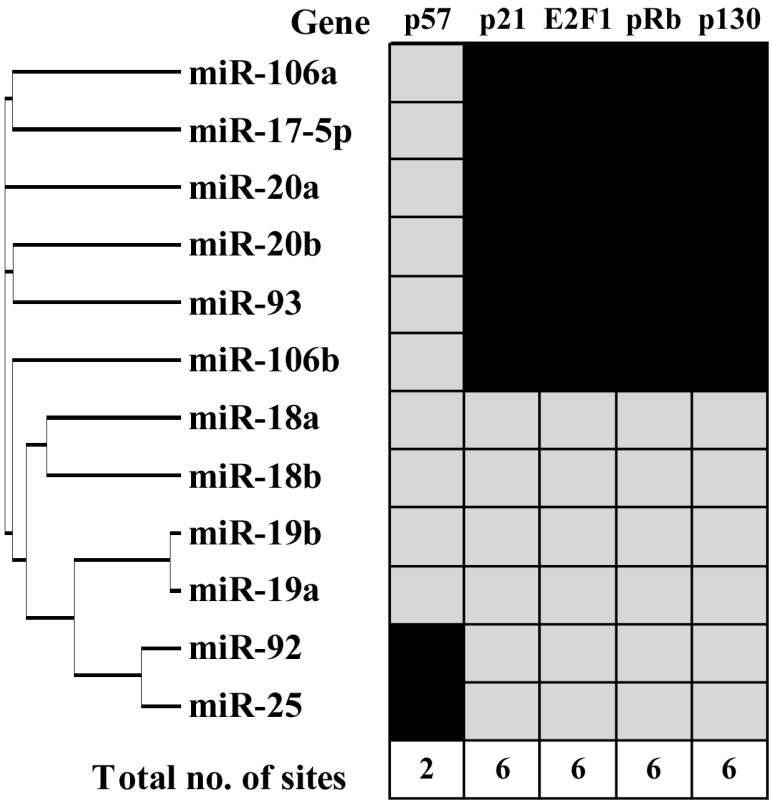

Figure S4. **miRNAs from the three paralogous polycistrons and their cell-cycle associated targets.**

Targeting of cell-cycle associated genes by miRNAs that belong to the miR-17-93, miR-106a-93 and miR-106b-25 polycistrons as predicted by PicTar. Black areas indicate predicted targeting.

Figure S5

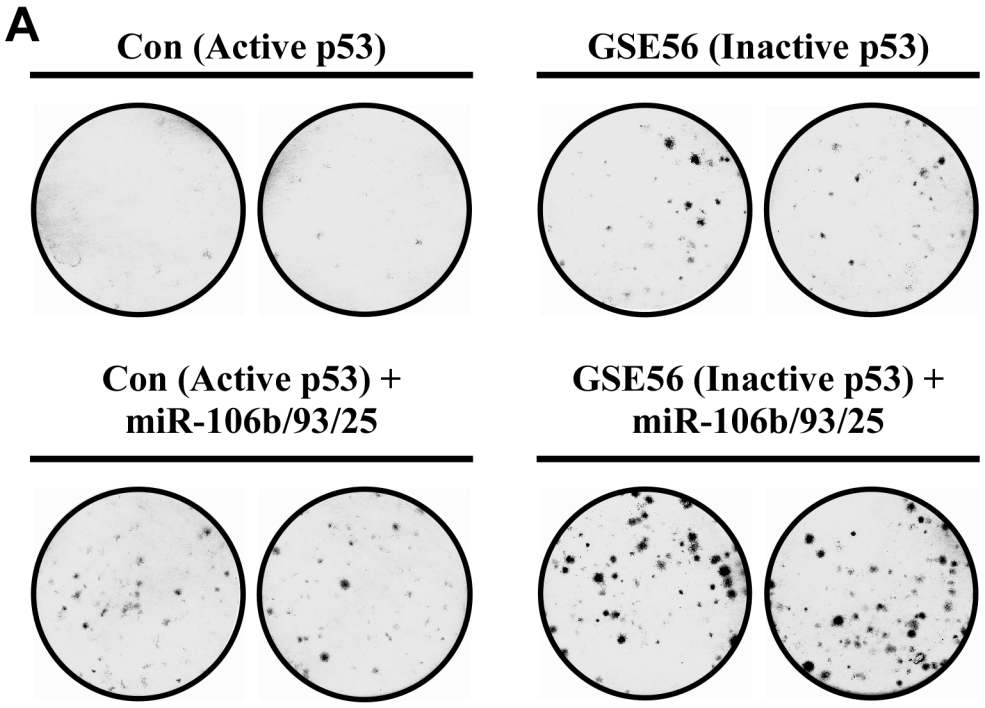
A
Con (Active p53)
GSE56 (Inactive p53)
Con (Active p53) +
miR-106b/93/25
GSE56 (Inactive p53) +
miR-106b/93/25

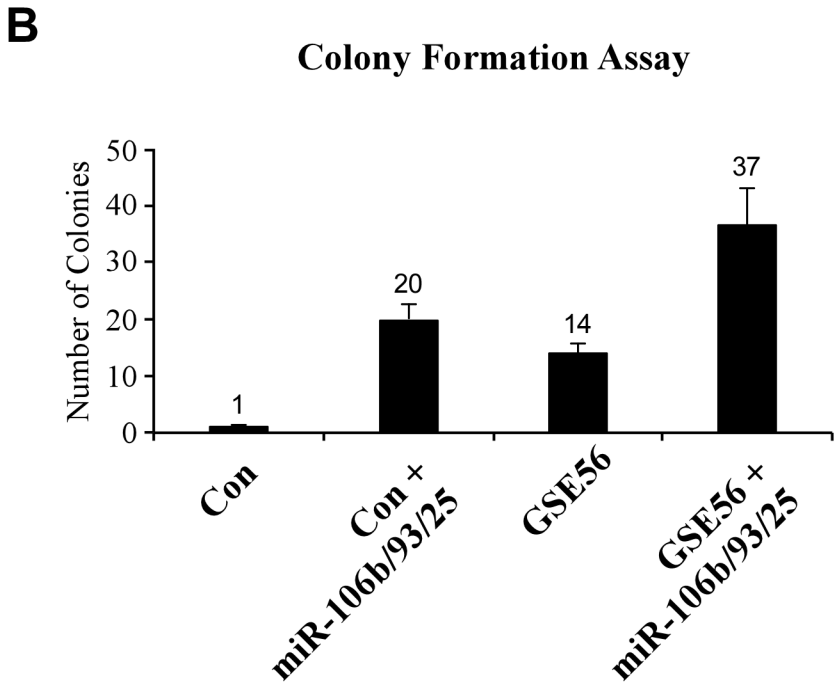
B
Colony Formation Assay
Number of Colonies
50
40
30
20
10
0
1
20
14
37
Con
Con +
miR-106b/93/25
GSE56
GSE56 +
miR-106b/93/25

Figure S5. **Effect of miR-106b/93/25 on colony formation efficiency in WI-38 cells in the presence and absence of GSE56.** WI-38 primary human fibroblasts were infected with a retrovirus encoding for the p53-inactivating peptide, GSE56. These cells and their active-p53 counterparts (Con) were infected with a retrovirus encoding for either the genomic region that contains miR-106b/93/25 or an empty vector control. After selection with the appropriate selection drug cells were plated (in duplicates) at low density and incubated for 10 days. A. Colonies were stained with crystal violet and plates were scanned. B. Colonies were counted. The average number of colonies (and standard deviation) for each condition are plotted. Note that the effect of miR-106b/93/25 overexpression in the control cells (that express an active p53) is more pronounced than in the GSE56-expressing cells.

Figure S6

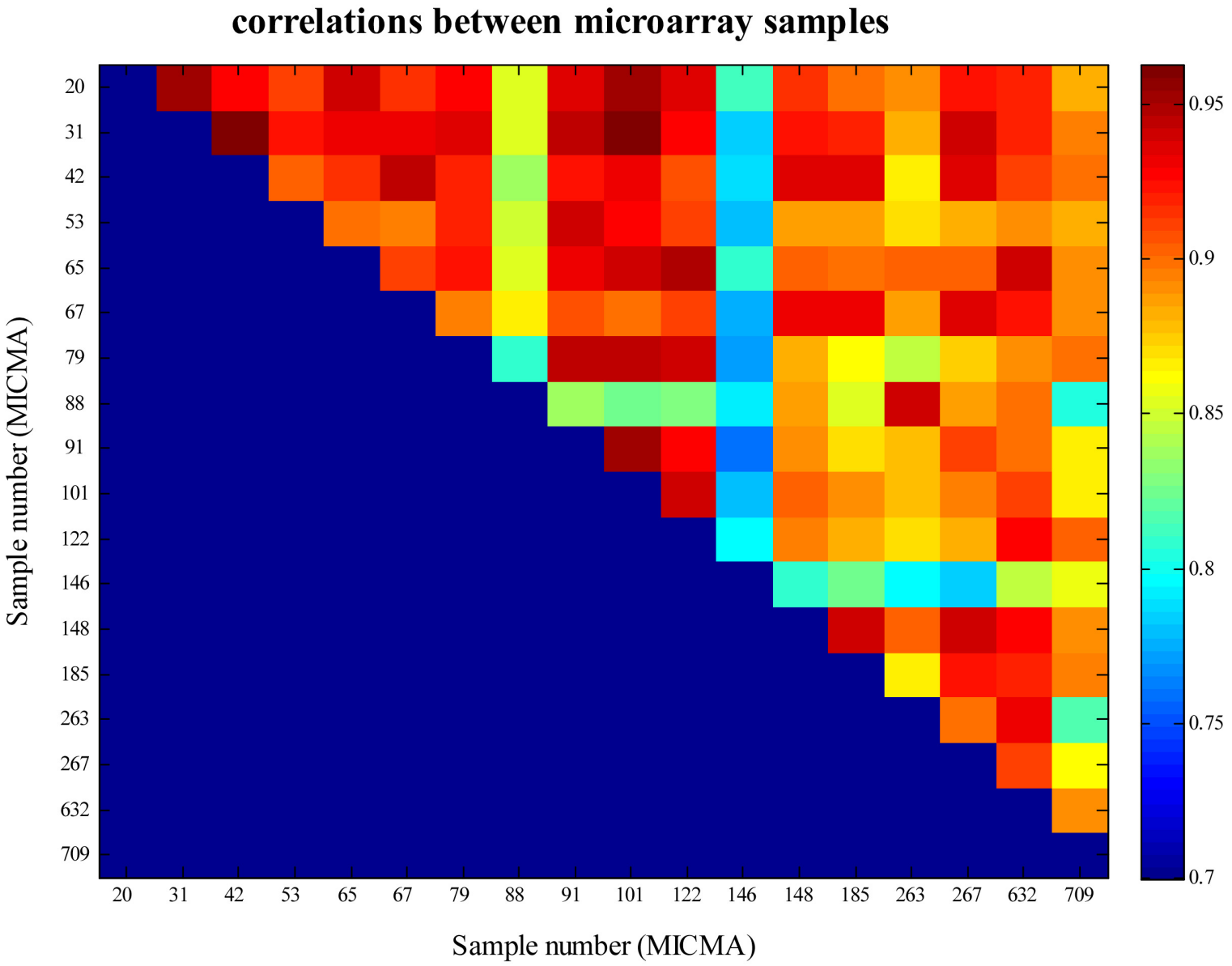

Figure S6. **Correlation coefficient between pairs of miRNA microarrays from the breast cancer study.**

Two samples, MICMA88 and MICMA146, were consistently more different from all other samples. Therefore, they were discarded from subsequent clustering analysis. These samples represent two out of 12 tumor samples with mutant p53.

Table S1. Detailed description of TP53 gene mutations and expression subtypes of the 16 breast cancer samples

Samples series: MicMa; Material: DNA, tumor; Method: Sequencing, TTGE; Region analysed: Exon 2-11; Reference sequence: NM_095720.

Sample ID	Expression Subgroup	TP53 status	Mutated Exon	Codon	Codon Change	Substitution	Mutation Type (predicted)	Codon 72 Polymorphism	Other variants, Polymorphism
31	Basal like	MUT	7	234	TAC>TGC	Tyr>Cys	Missense	G/G Arg/Arg	
42	Basal like	MUT	7	248	CGG>CAG	Arg>Gln	Missense	G/C Arg/Pro	c213, CGA>CGG, Arg>Arg,het
53	ERBB2	MUT	5	141	TGC>TAC	Cys>Tyr	Missense	G/G Arg/Arg	
67	Basal like	MUT	8	274	GTT>TTT	Val>Phe	Missense	G/G Arg/Arg	
79	ERBB2	MUT	6	209	Deletion of 2 bps		Frameshift	G/G Arg/Arg	
91	Luminal B	MUT	9		IVS9+1 G>A		Splice	G/C Arg/Pro	IVS4-29C>A,het
148	Luminal B	MUT	8	274	GTT>GAT	Val>Asp	Missense	G/G Arg/Arg	
185	Basal like	MUT	5	173	GTG>ATG	Val>Met	Missense	G/G Arg/Arg	
267	Basal like	MUT	6	213	CGA>TGA	Arg>Stop	Nonsense	G/G Arg/Arg	
709	Basal like	MUT	6	195/196	Deletion of 1 bp		Frameshift	G/C Arg/Pro	
20	Normal like	WT						G/G Arg/Arg	
65	Luminal A	WT						G/C Arg/Pro	
101	Luminal A	WT						G/G Arg/Arg	
122	Luminal A	WT						G/C Arg/Pro	
263	Luminal A	WT						G/G Arg/Arg	
632	Luminal A	WT						G/C Arg/Pro	

Table S2. miRNAs that were co-clustered with mRNAs enriched for distinct functional annotations

Cell-Cycle	Immune Response
miR-106a	miR-142-3p
miR-106b	miR-142-5p
miR-135b	miR-146b
miR-146a	miR-150
miR-15b	miR-155
miR-17-3p	miR-7
miR-17-5p	
miR-18a	
miR-18b	
miR-19a	
miR-19b	
miR-20a	
miR-20b	
miR-223	
miR-25	
miR-32	
miR-362	
miR-363	
miR-454-3p	
miR-500	
miR-502	
miR-532	
miR-545	
miR-576	
miR-579	
miR-590	
miR-660	
miR-9	
miR-9*	
miR-92	
miR-93	

Table S3. Functional annotation enrichment analysis for clustered genes derived from breast cancer samples.

A

Functional Annotation Term	No. of Cluster Genes	Enrichment P-Value
Mitotic cell cycle	39	8.53E-20
Cell cycle	70	1.11E-18
M phase	34	2.62E-16
Mitosis	28	3.13E-14
M phase of mitotic cell cycle	28	4.39E-14
Cell division	27	1.37E-11
Chromosome segregation	14	2.63E-11
Regulation of progression through cell cycle	40	4.86E-09
Regulation of cell cycle	40	5.16E-09
Cell cycle checkpoint	12	2.20E-08
Cell proliferation	41	8.27E-08
Cytoskeleton organization and biogenesis	34	1.09E-07
Organelle organization and biogenesis	53	3.77E-07
DNA metabolism	42	8.93E-06
Phosphoinositide-mediated signaling	12	1.76E-05
Mitotic sister chromatid segregation	7	2.24E-05
Sister chromatid segregation	7	3.01E-05
Microtubule-based process	17	4.50E-05
Interphase of mitotic cell cycle	10	5.62E-05
Interphase	10	7.32E-05
Response to DNA damage stimulus	21	8.10E-05
DNA-dependent DNA replication	12	8.23E-05
Ectoderm development	12	9.08E-05

B

Functional Annotation Term	No. of Cluster Genes	Enrichment P-Value
Immune response	92	1.24E-48
Response to biotic stimulus	97	2.12E-48
Defense response	94	5.36E-47
Response to pest, pathogen or parasite	56	2.52E-32
Response to other organism	56	5.97E-31
Response to stimulus	106	1.08E-28
Organismal physiological process	99	9.36E-27
Response to stress	60	4.50E-21
Response to virus	17	8.29E-15
Response to external stimulus	35	1.23E-14
Response to wounding	30	9.15E-14
Humoral immune response	20	7.40E-13
Inflammatory response	20	6.76E-11
Chemotaxis	16	1.20E-10
Taxis	16	1.20E-10
Locomotory behavior	16	2.10E-10
Regulation of apoptosis	24	4.29E-10
Regulation of programmed cell death	24	4.80E-10
Humoral defense mechanism	15	5.97E-10
Antimicrobial humoral response	13	2.77E-09
Cell death	29	4.28E-09
Death	29	4.96E-09
Apoptosis	28	8.01E-09
Programmed cell death	28	8.63E-09
Behavior	17	9.69E-09
Antimicrobial humoral response	12	2.03E-08
Calcium ion homeostasis	11	6.99E-08
Response to chemical stimulus	22	7.35E-08
Response to abiotic stimulus	23	1.84E-07
Lymphocyte activation	11	4.28E-07
Cell communication	79	5.67E-07
Signal transduction	74	8.96E-07
Cellular defense response	11	1.33E-06
Di-, tri-valent inorganic cation homeostasis	11	2.04E-06
Immune cell activation	11	2.22E-06
Cell activation	11	2.41E-06
Metal ion homeostasis	11	3.88E-06
Induction of programmed cell death	12	4.01E-06

Table S4. Conserved E2F sites predictions upstream of the three miRNA polycistrons

Predicted E2F sites were searched for in the genomic region spanning up to 10,000 bps upstream of the first miRNA in each polycistron (i.e. miR-17-5p, miR-106b and miR-106a), using the *tfbsConsSites database* (UCSC, human genome version hg17).

miRNA Polycistron	Chr	Site name	Position-Specific Scoring Matrix (PSSM)	Distance Upstream of first miRNA in the polycistron	Distance upstream from Primary Transcript/Host TSS	Site Sequence
hsa-mir-17-92	13	miR-17-92 site 1	V$E2F_Q3	2868	83	CCTTCGCGC
hsa-mir-106b-25	7	miR-106b-25 site 1	V$E2F_01	7513	814	ACCGCGGGAAACCCGG
hsa-mir-106b-25	7	miR-106b-25 site 2	V$E2F_01	7336	637	GACGTTTCGCGCCAAT
hsa-mir-106b-25	7	miR-106b-25 site 3	V$E2F4DP2_01	6821	129	GTTCCCGCG
hsa-mir-106a-92	X	miR-106a-92 site 1	V$E2F_Q3	3798	no known primary transcript	CTTCGCGCC

Table S5. Mutual targets of E2F transactivation and miR-106b/93/25 silencing

The list of E2F targets was compiled from a combination of seven high-throughput studies designed to identify E2F target genes (Ishida et al., 2001; Ma et al., 2002; Muller et al., 2001; Polager et al., 2002; Ren et al., 2002; Stanelle et al., 2002; Weinmann et al., 2001). Prediction of miRNA sites was performed using PicTar (Krek et al., 2005).

RefSeq	Symbol	Name	PicTar predicted sites		
NM_000076	CDKN1C	cyclin-dependent kinase inhibitor 1C	miR-25		
NM_000321	RB1	retinoblastoma 1	miR-93	miR-106b	
NM_001124	ADM	adrenomedullin	miR-25		
NM_001386	DPYSL2	dihydropyrimidinase-like 2	miR-93	miR-106b	
NM_001396	DYRK1A	dual-specificity tyrosine-(Y)-phosphorylation	miR-93	miR-106b	
NM_001430	EPAS1	endothelial PAS domain protein 1	miR-93	miR-106b	
NM_001450	FHL2	four and a half LIM domains 2 isoform 1	miR-25		
NM_001753	CAV1	caveolin 1	miR-106b		
NM_001769	CD9	CD9 antigen	miR-25		
NM_001949	E2F3	E2F transcription factor 3	miR-93	miR-106b	miR-25
NM_002024	FMR1	fragile X mental retardation 1	miR-25		
NM_002499	NEO1	neogenin homolog 1	miR-93		
NM_003016	SFRS2	splicing factor, arginine/serine-rich 2	miR-93	miR-106b	
NM_003139	SRPR	signal recognition particle receptor ('docking	miR-25		
NM_003272	TM7SF1	transmembrane 7 superfamily member 1	miR-106b		
NM_003505	FZD1	frizzled 1	miR-106b		
NM_003954	MAP3K14	mitogen-activated protein kinase kinase kinase	miR-93	miR-106b	
NM_004036	ADCY3	adenylate cyclase 3	miR-25		
NM_004354	CCNG2	cyclin G2	miR-93	miR-106b	

NM_004364	CEBPA	CCAAT/enhancer binding protein alpha	miR-25		
NM_004844	SH3BP5	SH3-domain binding protein 5 (BTK-associated)	miR-93	miR-106b	
NM_005197	CHES1	checkpoint suppressor 1	miR-106b		
NM_005458	GPR51	G protein-coupled receptor 51	miR-106b		
NM_005596	NFIB	nuclear factor I/B	miR-93	miR-25	
NM_005779	LHFPL2	lipoma HMGIC fusion partner-like 2	miR-25		
NM_005923	MAP3K5	mitogen-activated protein kinase kinase kinase	miR-93	miR-106b	
NM_006195	PBX3	pre-B-cell leukemia transcription factor 3	miR-106b		
NM_006352	ZNF238	zinc finger protein 238 isoform 2	miR-93	miR-106b	
NM_006482	DYRK2	dual-specificity tyrosine-(Y)-phosphorylation	miR-93	miR-25	
NM_006751	SSFA2	sperm specific antigen 2	miR-93	miR-106b	miR-25
NM_006806	BTG3	B-cell translocation gene 3	miR-93	miR-106b	
NM_012334	MYO10	myosin X	miR-106b		
NM_014344	FJX1	four jointed box 1	miR-93	miR-106b	
NM_014679	KIAA0092	translokin	miR-93	miR-106b	
NM_014876	KIAA0063	KIAA0063 gene product	miR-93	miR-106b	miR-25
NM_015008	KIAA0779	KIAA0779 protein	miR-93	miR-106b	
NM_015678	NBEA	neurobeachin	miR-93	miR-106b	
NM_016131	RAB10	ras-related GTP-binding protein RAB10	miR-93	miR-106b	
NM_016357	EPLIN	epithelial protein lost in neoplasm beta	miR-93	miR-106b	
NM_017803	FLJ20399	hypothetical protein FLJ20399	miR-25		
NM_021005	NR2F2	nuclear receptor subfamily 2, group F, member 2	miR-106b		
NM_053056	CCND1	cyclin D1	miR-93	miR-106b	
NM_057749	CCNE2	cyclin E2 isoform 1	miR-106b	miR-25	
NM_145725	TRAF3	TNF receptor-associated factor 3 isoform 1	miR-25		
NM_153719	NUP62	nucleoporin 62kDa	miR-93		

NM_173075	APBB2	amyloid beta A4 precursor protein-binding,	miR-93	miR-106b	
NM_173173	NR4A2	nuclear receptor subfamily 4, group A, member 2	miR-93	miR-106b	
NM_173200	NR4A3	nuclear receptor subfamily 4, group A, member 3	miR-93	miR-106b	miR-25
NM_174886	TGIF	TG-interacting factor isoform d	miR-25		
NM_181659	NCOA3	nuclear receptor coactivator 3 isoform a	miR-93	miR-106b	
NM_182744	NBL1	neuroblastoma, suppression of tumorigenicity 1	miR-93	miR-106b	
NM_183384	RNF13	ring finger protein 13 isoform 3	miR-106b		
NM_197968	ZNF198	zinc finger protein 198	miR-93		
NM_198966	PTHLH	parathyroid hormone-like hormone isoform 1	miR-93	miR-106b	
NM_199334	THRA	thyroid hormone receptor, alpha isoform 1	miR-93	miR-106b	
NM_024322	MGC11266	hypothetical protein MGC11266	miR-93	miR-106b	

Ishida, S., Huang, E., Zuzan, H., Spang, R., Leone, G., West, M., and Nevins, J.R. (2001). Role for E2F in control of both DNA replication and mitotic functions as revealed from DNA microarray analysis. Mol Cell Biol *21*, 4684-4699.

Krek, A., Grun, D., Poy, M.N., Wolf, R., Rosenberg, L., Epstein, E.J., MacMenamin, P., da Piedade, I., Gunsalus, K.C., Stoffel, M.*, et al.* (2005). Combinatorial microRNA target predictions. Nat Genet *37*, 495-500.

Ma, Y., Croxton, R., Moorer, R.L., Jr., and Cress, W.D. (2002). Identification of novel E2F1-regulated genes by microarray. Arch Biochem Biophys *399*, 212-224.

Muller, H., Bracken, A.P., Vernell, R., Moroni, M.C., Christians, F., Grassilli, E., Prosperini, E., Vigo, E., Oliner, J.D., and Helin, K. (2001). E2Fs regulate the expression of genes involved in differentiation, development, proliferation, and apoptosis. Genes Dev *15*, 267-285.

Polager, S., Kalma, Y., Berkovich, E., and Ginsberg, D. (2002). E2Fs up-regulate expression of genes involved in DNA replication, DNA repair and mitosis. Oncogene *21*, 437-446.

Ren, B., Cam, H., Takahashi, Y., Volkert, T., Terragni, J., Young, R.A., and Dynlacht, B.D. (2002). E2F integrates cell cycle progression with DNA repair, replication, and G(2)/M checkpoints. Genes Dev *16*, 245-256.

Stanelle, J., Stiewe, T., Theseling, C.C., Peter, M., and Putzer, B.M. (2002). Gene expression changes in response to E2F1 activation. Nucleic Acids Res *30*, 1859-1867.

Weinmann, A.S., Bartley, S.M., Zhang, T., Zhang, M.Q., and Farnham, P.J. (2001). Use of chromatin immunoprecipitation to clone novel E2F target promoters. Mol Cell Biol *21*, 6820-6832.

Table S6A. Primers used for quantification of mRNA levels (using QRT-PCR).

Gene Symbol , RefSeq No.	Forward Primer (5' to 3')	Reverse Primer (5' to 3')
GAPDH, NM_002046	agcctcaagatcatcagcaatg	cacgataccaaagttgtcatggat
MCM7, NM_005916	tctggcacgtctgagaatggt	acggacggtggcaaatatca
C13ORF25	gaagatggtggcggctactc	ggtgcagttaggtccacgtgtat
E2F1, NM_005225	ccatccaggaaaaggtgtgaa	agcgcttggtggtcagattc
CCNE1 (Cyclin E), NM_001238	tttacccaaactcaacgtgcaa	tcggagacctaccacgttatta
CDKN1A (p21), NM_078467	cgcgactgtgatgcgctaatg	ggaacctctcattcaaccgcc
CDKN1C (p57), NM_000076	gaacgccgaggaccagaac	ggcatgtcctgctggaagtc
RBL2 (p130), NM_005611	caagcaacctcagccttcca	ttctctccatctaaagttaccgaaga
CDC20, NM_001255	gagggtggctgggttcctct	cagatgcgaatgtgtcgatca
BIC	tgtgcgagcagagaatctaccttt	tggaggaagaaacaggcttagaa

Table S6B. Primers used for ChIP analysis (using QRT-PCR).

Primer pair name	Forward Primer (5' to 3')	Reverse Primer (5' to 3')
miR-106b-25 sites 1-2	gtgattggcttgcggctag	caatcggacaaggcggc
miR-106b-25 site 3	tcttaagggctctgggctcc	ggaatgcccaaaagcgc
miR-17-92	ttttatgctaatgagggagtggg	gctcccgcctcaacgtaa
miR-106a-92	gctgcagctgtaggacacaattaat	gctacatccgctcctcacaaa
β-actin	actggctcgtgtgacaaggc	cactccaaggccgctttaca
β-tubulin (NM_177987)	ggagctgatggagtcagtgatg	cagctctcagcctcctttctg